International Journal of Energy and Environmental Engineering
https://doi.org/10.1007/s40095-021-00439-4

ORIGINAL RESEARCH

The effective combination of zirconia superacid and zirconia-impregnated CaO in biodiesel manufacturing: Utilization of used coconut cooking oil (UCCO)

Erlin Purwita Sari[1,2] · Karna Wijaya[1] · Wega Trisunaryanti[1] · Akhmad Syoufian[1] · Hasanudin[3] · Wahyu Dita Saputri[4]

Received: 17 June 2021 / Accepted: 10 October 2021

Abstract
The present study reports the effective combination of zirconia superacid and zirconia-impregnated CaO in biodiesel manufacturing through the utilization of used coconut cooking oil. The acid catalyst was synthesized by the wet impregnation method combined with H_2SO_4 0.9 M. This mixture was calcined at 500 °C and yielding the highest catalyst acidity of 3.60 mmol g^{-1}. The free fatty acid (FFA) levels of UCCO then was reduced through the esterification process by varying the catalyst weight, UCCO-to-methanol mole ratio, calcination temperature, and reaction time. Optimum FFA level was achieved with 5% catalyst weight, 1:15 UCCO/methanol ratio, and 1.5 h reaction time with reduced FFA level to 0.42%. The Zr–CaO catalyst was synthesized using the reflux method through heating at 80 °C for 4 h, achieving the highest catalyst basicity, 27.78 mmol g^{-1}, at a condition of 1% (*w*/*w*) Zr–CaO and calcination temperature of 800 °C. This catalyst was then used in the transesterification reaction to produce biodiesel. Transesterification reaction was carried out by 5% catalyst weight and esterification product to methanol mole ratio of 1:20 for 1.5 h, yielding a conversion value of UCCO into biodiesel of 55.35%.

Keywords Biodiesel · Esterification · Transesterification · Acid–base catalyst · Used coconut cooking oil

Introduction

Energy security in Indonesia is expeditiously declining due to an imbalance in energy availability with the needs of its citizens. The same is also the case in most countries in the world. The exploration and exploitation of energy sources are still very dependent on petroleum resources, which are now increasingly scarce, and their reserves are depleting. Furthermore, the burning of fossil fuels produces pollutant gases such as SO*x*, NO*x*, etc. Thus, new alternative energy, which is more environmentally friendly and renewable, is needed to solve this energy problem [1]. Biodiesel poses itself as one of the said alternatives, having many advantages of being non-toxic, biodegradable, has a high flash point, has good lubrication, containing no sulfur and carcinogenic components [2, 3]. Biodiesel is made from renewable sources such as vegetable oils or animal fats and more easily decomposed compared to animal fossil fuels [4, 5].

Generally, biodiesel production involves homogeneous catalysts, but this treatment is susceptible to corrosion and difficulty of product separation [6]. Hence, the heterogeneous catalyst is more suitable for biodiesel production with the benefit of desirable economic value and profitability, as it can be easily separated, is non-corrosive, and can be regenerated [7]. Sulfated zirconia (SZ) or SO_4/ZrO_2 is an excellent material to be applied in making biodiesel. This is mainly related to its high catalytic activity and selectivity to esters when fatty acids react with various alcohols [8]. The SZ shows results that imply it is the most potent solid superacid [9]. CaO is a solid base catalyst that is often used for

✉ Karna Wijaya
karnawijaya@ugm.ac.id

1 Department of Chemistry, Faculty of Mathematics and Natural Science, Universitas Gadjah Mada, Yogyakarta, Indonesia

2 Research Center for Accelerator Technology, Research Organization for Nuclear Technology - National Research and Innovation Agency (BATAN-BRIN), Yogyakarta 55281, Indonesia

3 Department of Chemistry, Biofuel Research Group, Faculty of Mathematics and Natural Science, Universitas Sriwijaya, Inderalaya 30662, Indonesia

4 Research Center for Physics, National Research and Innovation Agency (BRIN), PUSPIPTEK, South Tangerang City 15314, Indonesia

Published online: 23 October 2021

transesterification in the manufacture of biodiesel. Several studies claim CaO combined with metal oxides such as MgO and ZnO can produce biodiesel with a higher % yield than the use of pure CaO, wherewith the selection of the suitable carrier largely determines the efficiency of heterogeneous catalysts in their application [10, 11]. Zirconia can be used as a catalyst for heterogeneous acids and bases because it is amphoteric [12]. Zirconia is, thus, considered appropriate to be combined with CaO as a heterogeneous base catalyst. Studies on the use of zirconia as acid and base catalyst combinations have previously been reported [1].

Therefore, the concept of using those combinations by using another precursor and raw material for UCCO conversion to biodiesel should provide a solution to increase the economic value of UCCO into biodiesel as well as a manifestation of support for green chemistry. This method is suitable for use in the conversion of UCCO into biodiesel because it is known that UCCO has a high FFA content. Raw materials with a fairly high content of free fatty acids (FFA) are not suitable for conventional biodiesel production processes due to the possibility of saponification reaction. By doing an esterification reaction at an early stage using SZ catalyst, FFA levels of raw oil material can be reduced as prevention toward potential saponification reactions in the transesterification reaction using a basic catalyst. By avoiding the saponification reaction, the conversion of UCCO into biodiesel in the second step reaction (transesterification) can be maximized because all the fatty acid content in UCCO can be converted into biodiesel. In this study, the heterogeneous acid catalyst SZ synthesized through wet impregnation method will be combined with the heterogeneous base catalyst ZCa synthesized via reflux method. Each of catalyst then consecutively used for the application of esterification reaction to reduce the FFA levels in UCCO to be less than 1%, followed by transesterification reaction to convert UCCO produced by esterification to biodiesel product.

Experimental

Instrumentation and materials

The materials used were ZrO_2 produced by Jiaozou Huasu Chemical Co., Ltd., chemicals produced by E-Merck, namely $ZrOCl_2{\cdot}8H_2O$, methanol, H_2SO_4, ammonium sulfate, oxalic acid, PP indicator, NaOH, and 37% HCl. Other materials were technical CaO and UCCO. The types of equipment used in this research were an analytical balance (KERN ABT 220-4 M, weighing capacity: 220 g, resolution: 0.1 mg), oven (Memmert), furnace (Carbolite), centrifuge (Thermo Scientific SL 16R, max speed: 15,200 rpm, min speed: 300 rpm), hot plate stirrer (AS ONE Magnetic REXIM RSH-1D, max temperature setting: 250 °C, rotation speed: 100–1500 rpm), and 1 set of reflux tool (Pyrex).

Identification and characterization supporting instruments used were Fourier Transform Infrared spectrophotometer (FTIR, Shimadzu Prestige-21, high signal-to-noise ratio: 40,000:1 or better, high sensitivity DLATGS Detector), X-Ray Diffraction diffractometer (X'Pert PRO PANalytical, elimination of Kβ (Ni filter), angle range from 0.2°, angular precision 0.001°), Scanning Electron Microscope combined with Energy Dispersive X-Ray (JEOL JSZ-6510 LA, resolutionHV mode: 3.0 nm (30 kV); 8 nm (3 kV); 15 nm (1 kV), Magnifications: × 5 to × 300,000 on 128 mm × 96 mm image size, Eucentric large specimen stage: X: 80 mm, Y: 40 mm, Z: 5 mm to 48 mm, Tilt: -10° to 90°, Rotation: 360°), Surface Area Analyzer (QUADROSORBTM-evo-MP/Kr, Surface Area Range: 0.01 m^2g^{-1} to no known upper limit (nitrogen), 0.0005 m^2g^{-1} to no known upper limit (krypton) Kr/MP model, Pore Size Range: 3.5 – 4000 Å, Minimum P/P_0 (N_2): 4×10^{-5}), Gas Chromatography Mass Spectroscopy (GC–MS Shimadzu QP2010S, mass range: *m/z* 1.5 to 1000, El scan sensitivity:: 1 pg octafluoronaphthalene *m/z* 272 S/N > 200, column flow: up to 4 mL/min), and Proton Nuclear Magnetic Resonance (^{1}H-NMR, JEOL ECZR 500, Frequency: 500 MHz, Magnetic strength: 11.5 T).

Synthesis of SZ catalyst

The SZ catalyst was synthesized using the wet impregnation method by mixing 10 g of ZrO_2 with 150 mL of H_2SO_4 solution with concentrations of 0.3, 0.6, and 0.9 M for 24 h. The mixture was then centrifuged for 15 min at 2000 rpm. The obtained solid was dried at 105 °C for 24 h, sieved with a size of 150 mesh, and calcined at 500 °C. The catalyst was labeled as 0.3 SZ, 0.6 SZ, and 0.9 SZ. Catalyst characterization was carried out using FTIR and acidity tests. Calcination at 400, 500, 600, and 700 °C to the SZ sample with maximum acidity was later performed for 4 h. The samples were labeled as SZ 400, SZ 500, SZ 600, and SZ 700. The XRD, FTIR, and acidity analysis were completed for each sample. The catalyst with maximum acidity was then characterized by Surface Area Analyzer and SEM–EDX to be used in the esterification stage.

UCCO preparation

The UCCO was heated at 105 °C to evaporate water and then filtered using filter paper. The determination of saponification number was done to obtain information on the molecular weight of the oil. The FFA level was determined by titration with three repetitions where 1 g of oil was added with 10 mL of methanol, heated to a temperature of 45 °C, added with PP indicator, and titrated using KOH that had

been standardized with oxalic acid ($H_2C_2O_4$). The equation is shown in Eq. (1) where sample mass is represented as W_{spl}

$$\text{FFA Level}(\%) = \frac{V_{KOH} \times N_{KOH} \times Mr_{\text{lauric acid}}}{W_{spl} \times 1000} \times 10 \quad (1)$$

Esterification of UCCO

The SZ catalyst with the highest acidity value was used in the esterification stage. Esterification was done to reduce free fatty acid content. At the esterification stage, there were several variations, namely variation in the weight of the catalyst to the total weight of methanol and UCCO (1, 5, and 5% (w/w), variation in the mole ratio of UCCO: methanol (1:5, 1:10, 1:15), and variation in reaction time (0.5, 1.0, 1.5 h). The fixed variable applied was UCCO weight, at 25 g. The reflux system was applied to the esterification process at 45 °C for 10 min, and then refluxed at 55 °C after the addition of UCCO.

Synthesis of base catalyst (Zr–CaO)

The Zr–CaO (ZCa) catalyst was made using reflux method with a concentration variation of 1, 5, 10, and 15% (*w*/*w*). The synthesis was carried out by refluxing ZrO_2 in the form of its precursor, namely $ZrOCl_2{\cdot}8H_2O$ with CaO and 100 mL aquabidest. The resulting products were evaporated to remove water, heated for 24 h at 120 °C, followed by sieving process to 150 mesh. The synthesized materials were labeled as 1 ZCa, 5 ZCa, 10 ZCa, and 15 ZCa and were characterized by FTIR and basicity test. Calcination for 4 h at 600, 700, 800, and 900 °C was performed to the catalyst with the highest basicity. The samples attained were labeled as ZCa-600, ZCa-700, ZCa-800, and ZCa-900. Subsequently, the catalysts were analyzed using XRD, FTIR, and basicity test. The material with maximum basicity underwent Surface Area Analyzer and SEM–EDX characterizations to be further applied to the esterification reaction.

Transesterification of the esterification product

The esterification product was transformed into biodiesel over the transesterification stage consuming the ZCa catalyst with maximum basicity. A total of 5% catalyst from methanol and UCCO mass was blended with methanol. By a ratio of 1:20, the mixture refluxed for 10 min at 45 °C, combined with the esterification product as much as 20 g, and reflux was continued at 55 °C for 90 min. To isolate the biodiesel product from the mixture, a centrifugation process at 3000 rpm was done for 15 min. The transesterification product was then cleaned from impurities using distilled water and anhydrous Na_2SO_4 to bind the remaining water. Transesterification results were analyzed using GC–MS to determine whether methyl esters had been formed along with ^{1}H-NMR to verify the amount of methyl ester conversion calculated based on the comparison between protons integration in triglycerides to the methoxy groups employing the Knothe equation [13].

$$C_{ME} = 100 \text{ x } \frac{5 \text{ x } I_{ME}}{5 \text{ x } I_{ME} + 9 \text{ x } I_{TG}}, \quad (2)$$

where C_{ME} conversion of triglyceride compounds into methyl esters (biodiesel) in the form of percentage; I_{ME}: the integration of methyl esters in H^1-NMR spectra; I_{TG}: the integration of triglyceride in H^1-NMR spectra.

Results and discussion

In this research, the synthesis of heterogeneous acid and base catalysts was done in which each catalyst played a role in the esterification and transesterification reaction, respectively, in the making of biodiesel from used coconut cooking (waste) oil. The zirconia-based catalysts consisting of SZ acid catalyst used in the esterification reaction and ZCa base catalyst used in the transesterification reaction were applied to produce biodiesel products. The SZ catalyst was synthesized by the wet impregnation method, while ZCa catalyst was synthesized by the reflux method.

Characterization of SZ heterogeneous acid catalyst

FTIR analysis

The SZ catalyst was synthesized by wet impregnation method at various H_2SO_4 concentrations, which were 0.3, 0.6, and 0.9 M. Furthermore, characterization was carried out with FTIR to determine changes in functional groups before and after the addition of H_2SO_4.

Figure 1 shows that in the ZrO_2 and SZ catalysts, there was a sharp absorption in the region of wavenumber 3448–3425 cm^{-1} denoted the stretching vibration of –OH group [4] and the water bending vibration (H–O–H) synchronized into the substance at wavenumber 1635 cm^{-1} [14]. At the absorption band of 748–501 cm^{-1}, the existence of Zr–O–Zr stretching vibrations was shown [15]. Some typical absorption bands that show the presence of sulfate groups appeared at wavenumbers 1226, 1157, 1080, and 1002 cm^{-1} which, respectively, represent the asymmetric vibration of S=O group, symmetrical vibration of S=O, SO asymmetric

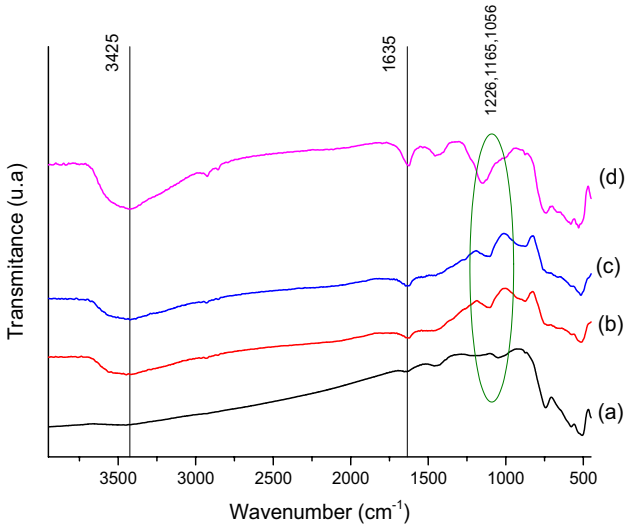

Fig. 1 FTIR spectra of **a** ZrO_2, **b** 0.3 SZ, **c** 0.6 SZ, and **d** 0.9 SZ

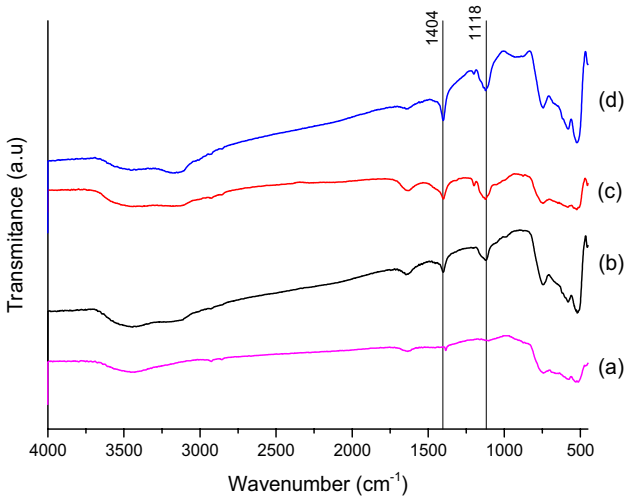

Fig. 2 FTIR spectra after acidity test of catalyst with concentration variation of **a** ZrO_2, **b** 0.3 SZ, **c** 0.6 SZ, and **d** 0.9 SZ

Table 1 Acidity value results of SZ catalyst at various H_2SO_4 concentrations

Catalyst	Acidity value (mmol g^{-1})
ZrO_2	1.42
0.3 SZ	1.90
0.6 SZ	2.18
0.9 SZ	2.87

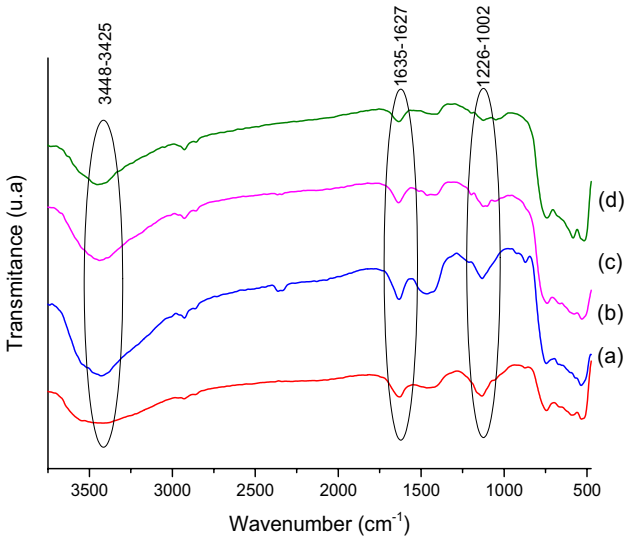

Fig. 3 FTIR result of calcination variations of **a** SZ 400, **b** SZ 500, **c** SZ 600, **d** SZ 700

vibration, and S=O symmetric vibration that indicates the binding of sulfate ions to the zirconium cation (Zr^{4+}) [1].

The analysis results of FTIR showed that the sharpest sulfate ion absorption band occurred at 0.9 SZ. This indicated that the highest H_2SO_4 concentration of 0.9 M is the optimum sulfate impregnation condition. Furthermore, an acid test was performed to determine the acidity value of the SZ catalyst using the gravimetric method. The catalyst, which had the highest acidity value, demonstrated that it had the best Brønsted acid and Lewis acid sites based on the amount of ammonia gas adsorbed by the catalyst [16]. Table 1 shows the ZrO_2 catalyst having an acidity value of 1.42 mmol g^{-1} originating from the zirconium cation Zr^{4+}. Zirconia impregnated with varying H_2SO_4 concentrations of 0.3, 0.6, and 0.9 M experienced an increase in acidity value, with the uppermost acidity of 2.87 mmol g^{-1} found in 0.9 M H_2SO_4 catalyst. This indicates that greater sulfate concentration impregnated on the zirconia surface can further increase the acid site on the catalyst [4].

Figure 2 shows the change in functional group absorbance in ZrO_2 and SZ after acidity testing at various concentrations of H_2SO_4. Absorbance at wavenumber 1118 cm^{-1} indicated the presence of NH_3 coordinated with the Lewis acid site, while a stretching vibration of 1404 cm^{-1} indicated the presence of $\mathbf{NH_4^+}$ ions formed through proton relocation from the Brønsted acid site to NH_3. The intensity of the ammonia absorption band found at the Lewis acid site, and the Brønsted acid site continued to increase at the 0.3 SZ, 0.6 SZ, and 0.9 SZ catalysts. Based on the FTIR data and acidity test, it was known that the 0.9 SZ catalyst was the catalyst that showed the highest acidity value. Thus, the sample was later given the calcination treatment with temperatures of 400, 500, 600, and 700 °C.

The effect of calcination temperature on the coordinated sulfate ion absorption bands on zirconium cations Zr^{4+} can be observed in Fig. 3. The intensity of sulfate group absorbance increased at calcination temperatures of 400 and 500 °C as can be observed through the sharp absorption at wavenumbers 1226, 1157, 1080, 1002 cm^{-1}. At temperatures of 600 and 700 °C, there was a decrease in the absorption of sulfate groups due to the desulfation or the release of sulfate from the zirconia surface under the influence of calcination heating [17].

This is reinforced by the results of the catalyst acidity test shown in Table 2.

The highest acidity value was demonstrated by the SZ 500 catalyst, with a value of 3.60 mmol g^{-1}. After the acidity test was done using ammonia, the SZ 500 catalyst showed the optimum NH_3 uptake, as shown by the FTIR spectra in Fig. 4. Optimum NH_3 absorption indicated that the catalyst had the most amount of acid sites. The FTIR analysis confirmed the results of the acidity test on the catalyst.

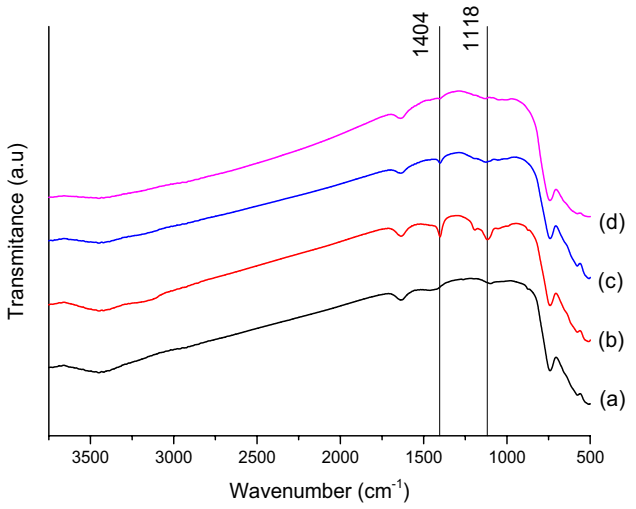

Fig. 4 FTIR spectra after acidity test of **a** SZ 400, **b** SZ 500, **c** SZ 600, **d** SZ 700

XRD analysis

The influence of temperature variation in calcination of the 0.9 SZ crystallinity is presented in Fig. 5. There were two peaks with the highest intensity, which were at 2Θ = 28.22° and 31.52° with respective d_{hkl} values of (d_{-111}) and (d_{111}) [18, 19].

The analysis showed that all samples still had the same crystalline phase, which was monoclinic. Changes occurred in intensities indicating the degree of material crystallinity. The decrease in intensity occurred at the SZ 500 where the intensity of the monoclinic peak was lower than that of the SZ 400. This phenomenon showed that sulfate ions were successfully impregnated and had covered the zirconia surface, causing the intensity of the monoclinic peak to decrease. However, as calcination temperatures increased at 600 °C and 700 °C, the intensity tended to increase. Increased temperatures at 600 °C and 700 °C caused sulfate ion decomposition, causing the monoclinic peak of ZrO_2 to again increase in intensity. Data related to 2Θ angles and d_{hkl} from the ZrO_2 monoclinic peaks are presented at ICSD PDF number 01–089-9066.

SEM–EDX analysis

SEM analysis results, presented in Fig. 6 did not show significant differences in the surface morphology of the ZrO_2 and SZ 500 catalysts. However, from these results, it appeared that the SZ 500 particle size looked larger than ZrO_2. This can be caused by the formation of sulfate agglomeration on the surface of the ZrO_2 catalyst [20]. The EDX analysis results in Table 3 show that the amount of S and O elements

Table 2 Acidity test results of SZ catalyst at various calcination temperatures

Catalyst	Acidity value (mmol g^{-1})
SZ 400	2.77
SZ 500	3.60
SZ 600	2.96
SZ 700	2.68

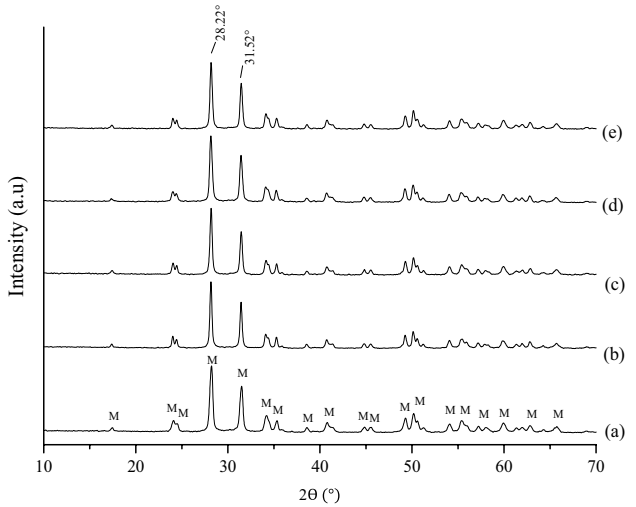

Fig. 5 Diffractogram of **a** SZ 400, **b** SZ 500, **c** SZ 600, **d** SZ 700

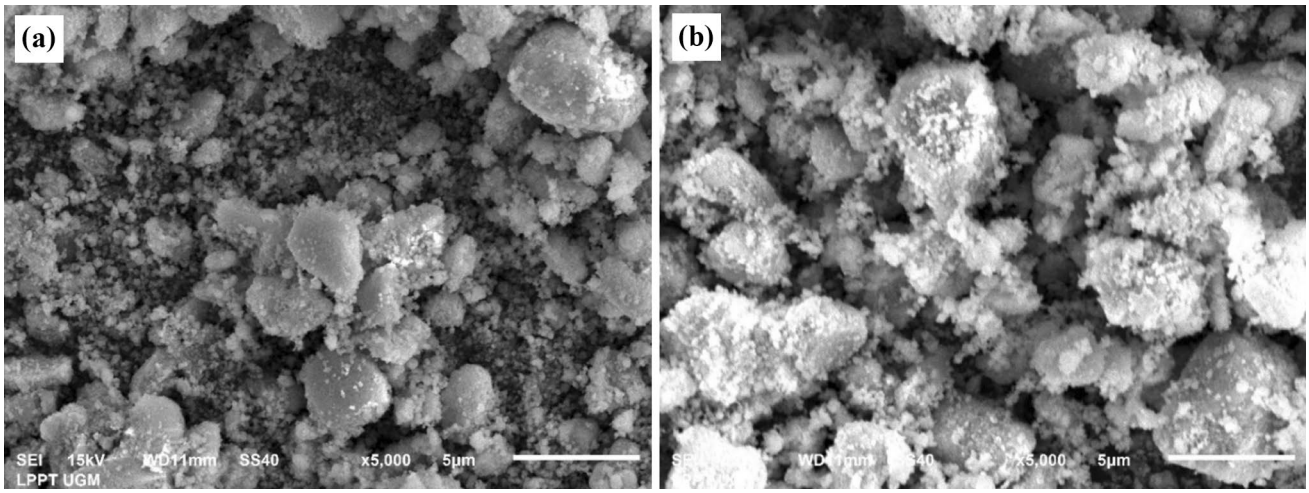

Fig. 6 SEM Analysis results of **a** ZrO_2 with magnification of 5000×, **b** ZS-500 with magnification of 5000×

Table 3 Results of EDX analysis for ZrO_2 and SZ 500

Catalyst	Mass (%)		
	Zr	O	S
ZrO_2	70.53	29.04	0.43
SZ 500	59.44	38.93	1.62

Table 4 Results of surface area analyzer analysis

Catalyst	Surface Area ($m^2\ g^{-1}$)	Average Pore Diameter (nm)	Total Pore Volume ($cm^3\ g^{-1}$)
ZrO_2	5.89	22.43	0.03
SZ 500	4.86	29.37	0.03

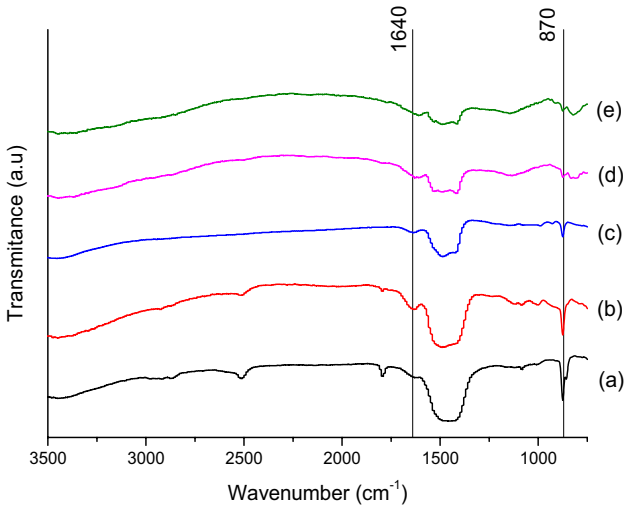

Fig. 7 FTIR spectra of **a** CaO, **b** 1 ZCa, **c** 5 ZCa, **d** 10 ZCa, **e** 15 ZCa

had increased after the sulfation of ZrO_2. This indicated that the sulfate ion was successfully impregnated onto ZrO_2.

SAA (surface area analyzer) analysis

The SZ 500 catalyst showed a smaller surface area than ZrO_2. This is in accordance with the results of SEM analysis which displayed a larger particle size on the catalyst surface. Reductions in the surface area of catalysts with higher sulfur content can also occur due to the migration of sulfates into bulk solids [21]. The average pore diameter and total pore volume experienced increases, possibly due to the damage to the opening of the zirconia pores due to acid treatment. The results of the Surface Area Analyzer analysis are shown in Table 4.

Despite the decrease in surface area, the SZ 500 catalyst had a large average pore diameter of 29.37 nm, meaning that it can easily adsorb fatty acid molecules which have a pore diameter of around 2.50 nm. Under these conditions, the reaction can take place at the entire active site of the catalyst, both on the external and internal surfaces of the catalyst [22]. Modeling using the DFT method was recommended for use in SAA analysis to perform pore analysis. From the modeling, it was known that ZrO_2 had

Table 5 ZCa catalyst basicity test results at various Zr concentrations

Catalyst Sample	Total Basicity (mmol g^{-1})
CaO	20.20
1 ZCa	27.78
5 ZCa	22.73
10 ZCa	16.84
15 ZCa	15.99

a cylindrical shape, and there was a gap that allowed the impregnation of sulfate ions.

Characterization of ZCa heterogeneous catalyst

FTIR analysis

The ZCa catalyst was synthesized using the reflux method with heating at 80 °C for 4 h with varying ZCa weights of 1, 5, 10, and 15% (w/w). The synthesized catalyst materials were then characterized by FTIR. Figure 7 shows the CaO and ZCa catalyst absorbance at various concentrations. Absorption in the regions of 3643, 1640, and 870 cm^{-1}, respectively, represented -OH stretching vibration, OH bending vibration, and vibration of water adsorbed on the surface of CaO [23]. FTIR spectra showed the same pattern in each variation of concentration but demonstrated a change in intensity. The higher concentration of Zr used caused the intensity of the absorption band typical of CaO to decrease. The higher concentration of Zr onto CaO impregnated resulted in a decrease in the characteristic of the absorption bands possessed by CaO.

Basicity test with the titration method was carried out to determine quantitatively the number of basic sites found on the ZCa catalyst at various concentrations. Table 5 shows that CaO had an alkaline site of 20.20 mmol g^{-1}, originating from the O^{2-} Lewis base.

The addition of $ZrOCl_2{\cdot}8H_2O$ precursor to CaO can produce new crystals including monoclinic ZrO_2, $CaZrO_3$ (orthorhombic) phases, and tetragonal ZrO_2. The formation of $CaZrO_3$ crystal contributed to the basicity of the catalyst. Compared with monoclinic and tetrahedral ZrO_2 crystals, $CaZrO_3$ crystal has higher basicity. The basic nature of CaO-ZrO_2 is a result of the free CaO aggregate base site and the surface of $CaZrO_3$ [24]. The highest total alkalinity was found in catalyst 1 ZCa, with a total alkalinity of 27.78 mmol g^{-1}. At higher Zr concentrations, the basicity of catalyst decreased since the growth of ZrO_2 crystal inhibited the formation of $CaZrO_3$, which contributes to the basicity of solids [23].

The consequence of calcination observed by FTIR analysis and the absorption band can be seen in Fig. 8. The region at the wavenumber 750–509 cm^{-1} showed the vibration

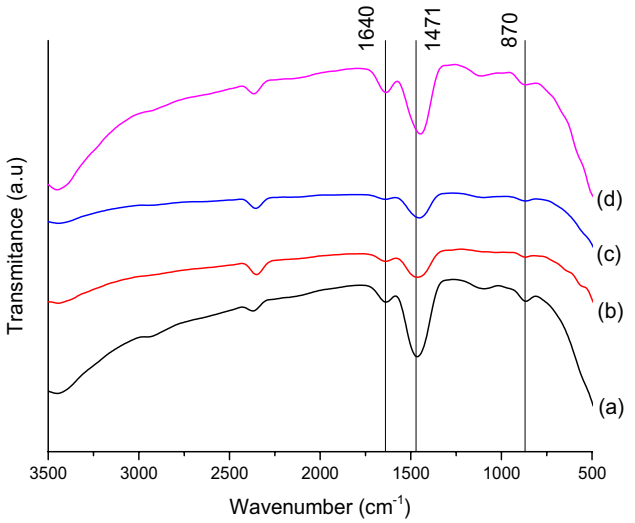

Fig. 8 FTIR spectra of **a** ZCa-600, **b** ZCa-700, **c** ZCa-800, **d** ZCa-900

Table 6 ZCa catalyst basicity test results of catalyst with various calcination temperatures

Catalyst Sample	Total Basicity (mmol g^{-1})
ZCa-600	20.62
ZCa-700	22.72
ZCa-800	23.99
ZCa-900	21.46

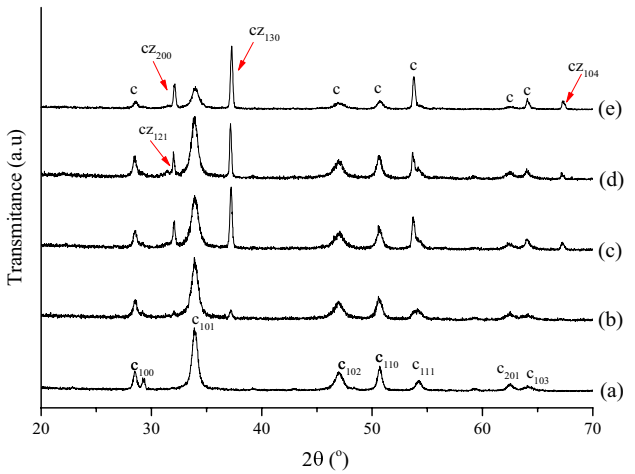

Fig. 9 Diffractogram of **a** ZCa-600, **b** ZCa-700, **c** ZCa-800, **d** ZCa-900

absorption of Zr–O. FTIR results show that as the calcination temperature increased from 600 to 800 °C, the characteristic of the CaO absorption band decreased in intensity and later returned at 900 °C. Impregnation of Zr in CaO can

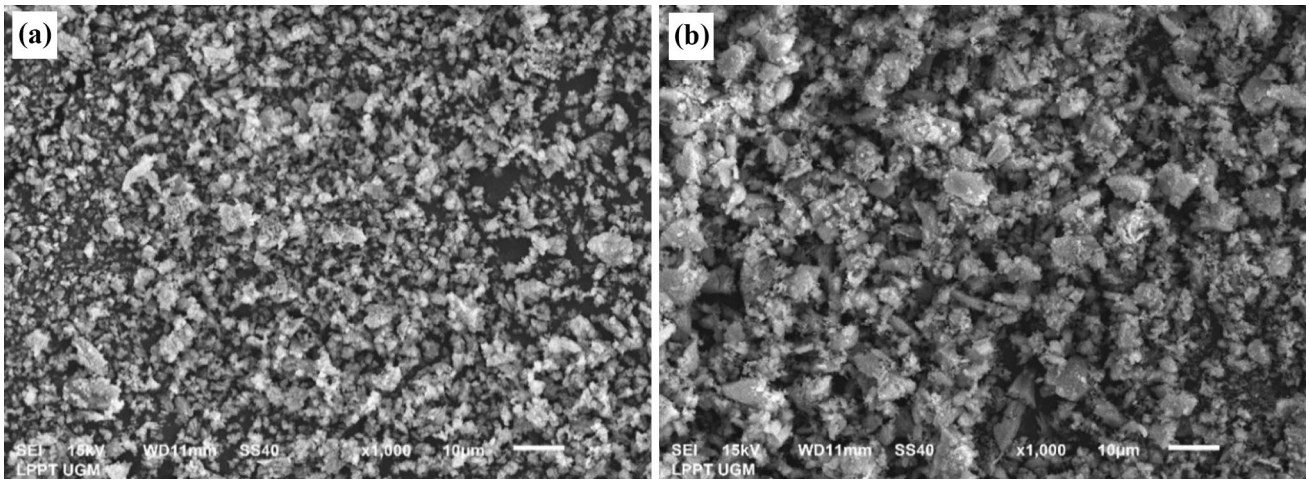

Fig. 10 SEM Analysis results of **a** CaO with magnification of 1000×, **b** ZCa-800 with magnification of 1000×

Table 7 Results of EDX analysis for CaO and ZCa-800

Catalyst	Mass (%)		
	Ca	O	Zr
CaO	42.30	53.09	4.61
ZCa-800	42.49	51.50	6.01

Table 8 Results of surface area analyzer analysis

Catalyst	BET Surface Area ($m^2\ g^{-1}$)	Average Pore Diameter (nm)	Total Pore Volume ($cm^3\ g^{-1}$)
ZrO_2	122.39	7.87	0.24
ZCa-800	107.50	7.87	0.21

form Ca-O-Zr hetero-linkage bonds or is stable for $CaZrO_3$ species [1].

From the results of the FTIR characterization and basicity test, the optimum catalyst was ZCa-800. Basicity test results are shown in Table 6.

XRD

The effect of calcination temperature variation on the crystallinity of 1 ZCa is presented in Fig. 9.

The structure of the catalyst material was studied using the X-ray Diffraction method. The effect of calcination temperature on the structure of the catalyst material was studied through variation in calcination temperature in the range of 600–900 °C using a reaction condition at a concentration of 1%. Figure 9 demonstrate that there was a decrease in peak intensity of $Ca(OH)_2$ and also the formation of new peaks in the diffraction pattern. At 600 °C, a new peak was formed at 31.98° which is characteristic to the $CaZrO_3$ crystal and increased significantly at 700 °C. Quantitative data of XRD analysis showed that the relative intensity of the peak displayed the highest value at 800 °C. This supports the results of basicity analysis, where the temperature variation of the catalyst had the highest basicity value.

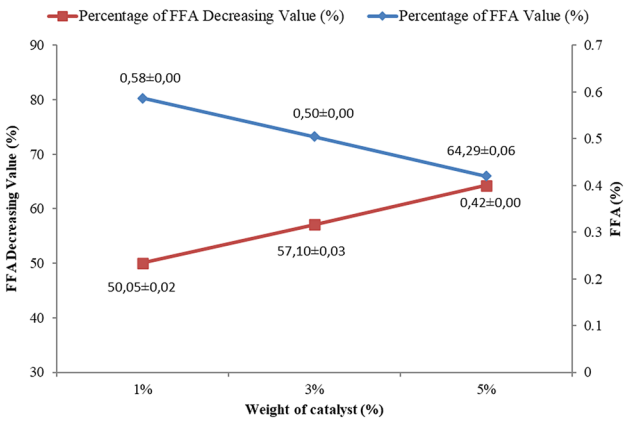

Fig. 11 FFA values obtained based on the catalyst weight variation of 1%, 3%, and 5%

SEM–EDX analysis

The presence of zirconia impregnated onto CaO might cause agglomeration on the CaO surface and thus resulting in larger particle size after impregnation as shown in Fig. 10.

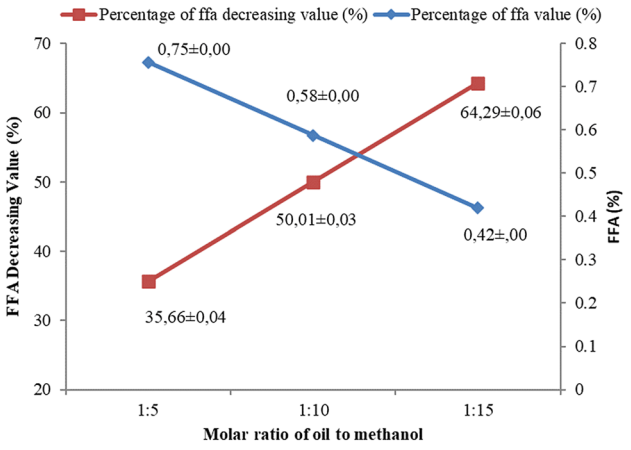

Fig. 12 FFA values obtained based on the variation of oil molar ratio to methanol

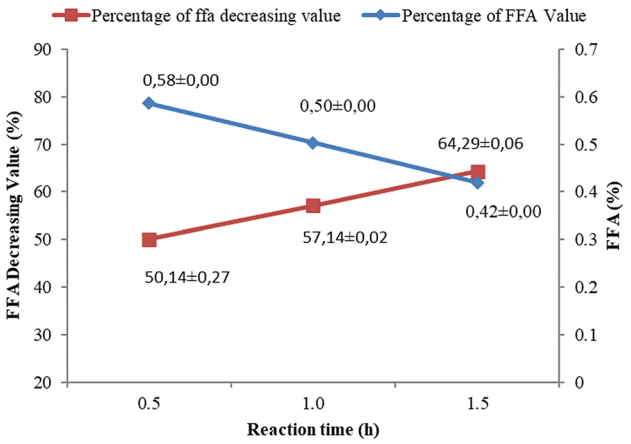

Fig. 13 FFA values obtained based on the variation of reaction time

The successful impregnation of Zr^{4+} cations on CaO catalysts was further proven by the results of the EDX analysis presented in Table 7 which showed that the Zr content of ZCa catalysts had increased.

SAA (surface area analyzer) analysis

The ZCa-800 catalyst showed a smaller surface area than CaO as presented in Table 8 and in line with to the results of SEM analysis which showed a larger particle size of ZCa. However, this catalyst had a higher basicity value than CaO. It was known that the catalytic activity of the base catalysts was more influence by its basic nature rather than the surface area of the catalyst.

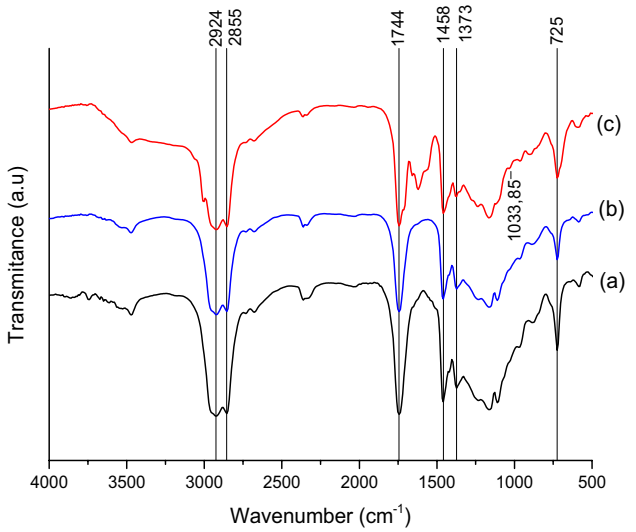

Fig. 14 FTIR spectra of **a** Used cooking oil, **b** Esterification product, and **c** Transesterification Product

Esterification application

The FFA level suitable for transesterification to be carried out without causing a saponification reaction to take place is under 1% [25]. The results of FFA reduction using catalysts from several variations are shown in Fig. 11, Fig. 12, and Fig. 13.

FTIR analysis results of esterification products

The FTIR analysis results in Fig. 14 showed several peaks of UCCO and transesterification product. The vibration at 1373 cm^{-1} appeared in all three samples. This vibration indicated the presence of the $O-CH_2$ group derived from triglycerides in UCCO.

Table 9 Area and retention time of GC analysis

Peak number	Compound	Molar weight (g mol^{-1})	Retention Time (min)	Area (%)
1	Methyl Octanoate	158	16.68	7.19
2	Methyl Decanoate	186	22.95	5.56
3	Methyl Laurate	214	28.47	48.41
4	Methyl Myristate	242	33.33	18.55
5	Methyl Palmitate	270	37.73	10.82
6	Methyl Palmitoleate	266	41.12	0.47
7	Methyl Oleate	296	41.25	5.71
8	Methyl Stearate	298	41.74	3.28

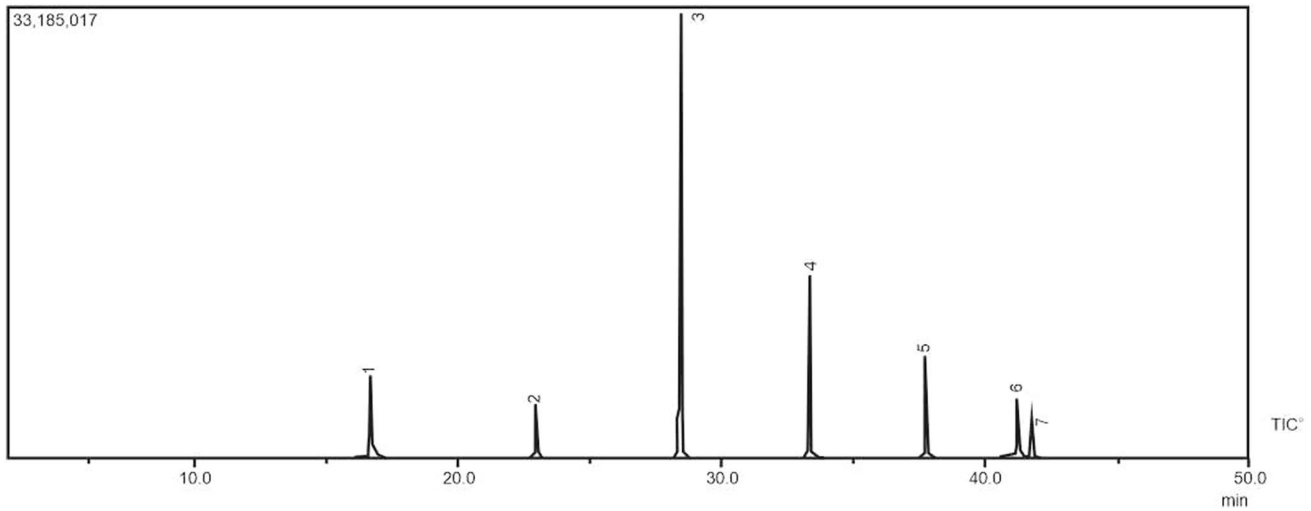

Fig. 15 Chromatogram of transesterification product

Though, on the transesterification product, this vibration indicated the presence of the $O-CH_2$ group in glycerol which was a byproduct of the reaction. The success in making biodiesel was shown by the emergence of a new peak at wavenumber 1034 cm^{-1} which is typical of the $O–CH_2–C$ vibration of the biodiesel compound [26].

GC–MS Analysis

The GC–MS chromatogram in Fig. 15 shows the composition of compounds making up the product of the transesterification reaction. The chromatogram shows that there were eight peaks identified as methyl ester compounds representing that there were eight methyl esters included in the biodiesel, which is presented in Table 9. From the results of GC analysis, it was known that the dominant compounds in the transesterification product were methyl laurate (48.41) and methyl myristate (18.55).

^{1}H-NMR Analysis

Figure 16 shows that there was doublet of doublet peaks that appeared at $\delta = 4.1$ and 4.3 ppm. The peak in this area indicated the existence of triglycerides proton [27], with an integration value of 1.38. In Fig. 17 protons from triglycerides did not reappear at all. This change indicated that the triglycerides had been transformed to methyl esters.

At the chemical shift $\delta = 3.62$ ppm, there was a singlet peak with a large relative abundance belonging to the proton from the methoxy group ($–OCH_3$). The characteristic peak in biodiesel is methoxy peak, existing at 3.62 ppm with an integration value of 3.08. In this study, the Knothe equation (Eq. 2) was used, incorporating the integrations of triglycerides and methyl esters from the ^{1}H-NMR, and a biodiesel conversion of 55.35% was calculated. Biodiesel conversion can be influenced by several factors including the kind and precursor of catalyst, catalyst weight, ratio of oil to alcohol, time, and reaction.

Conclusion

The heterogeneous acid catalyst SZ was successfully synthesized using a wet impregnation process of ZrO_2 and H_2SO_4 at room temperature (27–28 °C). The highest total acidity was 3.60 mmol g^{-1}, found on 0.9 M SZ 500 catalyst. Furthermore, the heterogeneous base catalyst ZCa was completely synthesized via a reflux method by employing CaO and $ZrOCl_2{\cdot}8H_2O$ pro analytical grade as a precursor. The optimum condition was reached using 1% weight of catalyst and calcination temperature of 800 °C (ZCa-800), yielding the total basicity of 27.78 mmol g^{-1}.

The SZ-500 catalyst was successfully applied in the esterification reaction of UCCO under the reaction condition: 5% weight of the catalyst, the mole ratio of oil to methanol of 1:15, the reaction time of 1.5 h, and temperature of 65 °C. By those reaction conditions, the FFA level was effectively reduced from 1.17% to 0.42%. In addition, the transesterification reaction was carried out by 5% ZCa-800 catalyst weight and esterification product to methanol mole ratio of 1:20 for 1.5 h. The high FFA UCCO, previously considered unused waste, has been successfully converted into biodiesel by 55.35%.

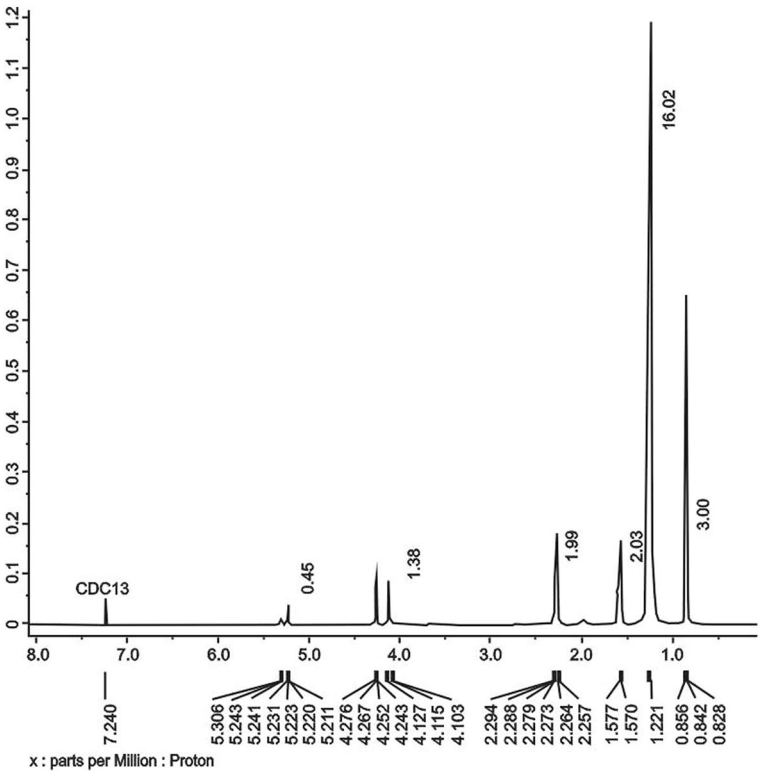

Fig. 16 [1]H-NMR spectra of UCCO

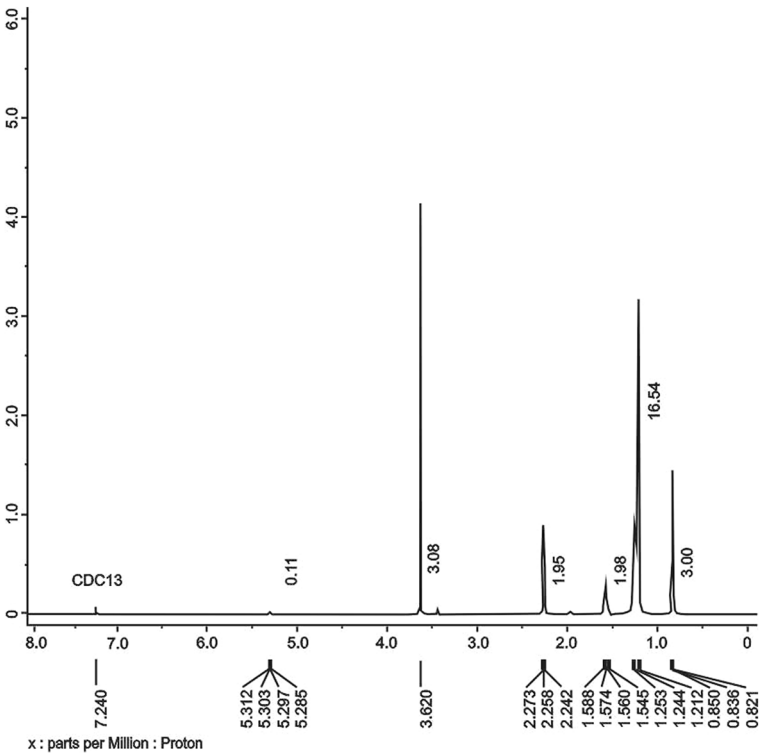

Fig. 17 [1]H-NMR spectra of biodiesel

Acknowledgements This research was supported by grant from the DRPM DIKTI fund for scientific research PTUPT 2019 (No. 2737/UN1.DITLIT/DIT-LIT/LT/2019) and Hibah Penelitian Thesis Magister (PTM) 2020.

Author Contribution All authors have contributed equally.

Declarations

Conflict of Interest The authors declare no conflict of interest.

References

1. Kaur, N., Ali, A.: Kinetics and reusability of Zr/CaO as heterogeneous catalyst for the ethanolysis and methanolysis of Jatropha crucas oil. Fuel Process. Technol. **119**, 173–184 (2014). https://doi.org/10.1016/j.fuproc.2013.11.002
2. Sibarani, J., Khairi, S., Yoeswono, Y., Wijaya, K., Tahir, I.: Effect of Palm Empty Bunch Ash on Transesterification of Palm Oil Into Biodiesel. Indones. J. Chem. **7**(3), 314–319 (2010). https://doi.org/10.22146/ijc.21675
3. Banković-Ilić, I.B., Miladinović, M.R., Stamenković, O.S., Veljković, V.B.: Application of nano CaO–based catalysts in biodiesel synthesis. Renew. Sustain. Energy Rev. **72**, 746–760 (2017). https://doi.org/10.1016/j.rser.2017.01.076
4. Patel, A., Brahmkhatri, V., Singh, N.: Biodiesel production by esterification of free fatty acid over sulfated zirconia. Renew. Energy **51**, 227–233 (2013). https://doi.org/10.1016/j.renene.2012.09.040
5. Pratama, L., Yoeswono, Y., Triyono, T., Tahir, I.: Effect of temperature and speed of stirrer to biodiesel conversion from coconut oil with the use of palm empty fruit bunches as a heterogeneous catalyst. Indones. J. Chem. **9**(1), 54–61 (2010). https://doi.org/10.22146/ijc.21562
6. Binti Mohd Alias, N.S., Veny, H., Hamzah, F., Aziz, N.: Effect of free fatty acid pretreatment to yield, composition and activation energy in chemical synthesis of fatty acid methyl ester. Indones. J. Chem. **19**(3), 592–598 (2019)
7. Marchetti, J.M., Miguel, V.U., Errazu, A.F.: Techno-economic study of different alternatives for biodiesel production. Fuel Process. Technol. **89**(8), 740–748 (2008). https://doi.org/10.1016/j.fuproc.2008.01.007
8. Jacobson, K., Gopinath, R., Meher, L.C., Dalai, A.K.: Solid acid catalyzed biodiesel production from waste cooking oil. Appl. Catal. B Environ. **85**(1–2), 86–91 (2008). https://doi.org/10.1016/j.apcatb.2008.07.005
9. Fraenkel, D., Jentzsch, N.R., Starr, C.A., Nikrad, P.V.: Acid strength of solids probed by catalytic isobutane conversion. J. Catal. **274**(1), 29–51 (2010). https://doi.org/10.1016/j.jcat.2010.06.002
10. Molaei Dehkordi, A., Ghasemi, M.: Transesterification of waste cooking oil to biodiesel using Ca and Zr mixed oxides as heterogeneous base catalysts. Fuel Process. Technol. **97**, 45–51 (2012). https://doi.org/10.1016/j.fuproc.2012.01.010
11. Tian, X., Xiao, T., Yang, C., Zhou, Z., Ke, H.: Synthesis of crystalline ordered mesoporous CaO-ZrO2 solid solution as a promising solid base. Mater. Chem. Phys. **124**(1), 744–747 (2010). https://doi.org/10.1016/j.matchemphys.2010.07.050
12. Wan Omar, W.N.N., Saidina Amin, N.A.: Optimization of heterogeneous biodiesel production from waste cooking palm oil via response surface methodology. Biomass Bioenergy **35**(3), 1329–1338 (2011). https://doi.org/10.1016/j.biombioe.2010.12.049
13. Knothe, G.: Monitoring a progressing transesterification reaction by fiber-optic near infrared spectroscopy with correlation to 1H nuclear magnetic resonance spectroscopy. J. Am. Oil Chem. Soc. **77**(5), 489–493 (2000)
14. Ardizzone, S., Bianchi, C.L., Cappelletti, G., Porta, F.: Liquid-phase catalytic activity of sulfated zirconia from sol-gel precursors: The role of the surface features. J. Catal. **227**(2), 470–478 (2004). https://doi.org/10.1016/j.jcat.2004.07.030
15. Kuwahara, Y., Fujitani, T., Yamashita, H.: Esterification of levulinic acid with ethanol over sulfated mesoporouszirconosilicates: Influences of the preparation conditions on the structural properties and catalytic performances. Catal. Today **237**, 18–28 (2014). https://doi.org/10.1016/j.cattod.2013.11.008
16. Hauli, L., Wijaya, K., Armunanto, R.: Preparation and characterization of sulfated zirconia from a commercial zirconia nanopowder. Orient. J. Chem. **34**(3), 1559–1564 (2018). https://doi.org/10.13005/ojc/340348
17. Rachmat, A., Trisunaryanti, W., Sutarno, K.W.: Synthesis and characterization of sulfated zirconia mesopore and its application on lauric acid esterification. Mater. Renew. Sustain. Energy **6**(3), 1–9 (2017). https://doi.org/10.1007/s40243-017-0097-1
18. Li, E., Xu, Z.P., Rudolph, V.: MgCoAl-LDH derived heterogeneous catalysts for the ethanol transesterification of canola oil to biodiesel. Appl. Catal. B Environ. **88**(1–2), 42–49 (2009). https://doi.org/10.1016/j.apcatb.2008.09.022
19. Takase, M., et al.: Application of zirconia modified with KOH as heterogeneous solid base catalyst to new non-edible oil for biodiesel. Energy Convers. Manag. **80**, 117–125 (2014). https://doi.org/10.1016/j.enconman.2014.01.034
20. Utami, M., Wijaya, K., Trisunaryanti, W.: Effect of sulfuric acid treatment and calcination on commercial zirconia nanopowder. Key Eng. Mater. **757**, 131–137 (2017)
21. Petchmala, A., et al.: Transesterification of palm oil and esterification of palm fatty acid in near- and super-critical methanol with SO4-ZrO2 catalysts. Fuel **89**(9), 2387–2392 (2010). https://doi.org/10.1016/j.fuel.2010.04.010
22. Essamlali, Y., Amadine, O., Larzek, M., Len, C., Zahouily, M.: Sodium modified hydroxyapatite: Highly efficient and stable solid-base catalyst for biodiesel production. Energy Convers. Manag. **149**, 355–367 (2017). https://doi.org/10.1016/j.enconman.2017.07.028
23. Zhang, Q., Zhang, Y., Li, H., Gao, C., Zhao, Y.: Heterogeneous CaO-ZrO2 acid-base bifunctional catalysts for vapor-phase selective dehydration of 1,4-butanediol to 3-buten-1-ol. Appl. Catal. A Gen. **466**, 233–239 (2013). https://doi.org/10.1016/j.apcata.2013.06.020
24. Xia, S., Guo, X., Mao, D., Shi, Z., Wu, G., Lu, G.: Biodiesel synthesis over the CaO-ZrO2 solid base catalyst prepared by a urea-nitrate combustion method. RSC Adv. **4**(93), 51688–51695 (2014). https://doi.org/10.1039/c4ra11362d
25. Anantapinitwatna, A., Ngaosuwan, K., Kiatkittipong, W., Wongsawaeng, D., Assabumrungrat, S.: Effect of Water Content in Waste Cooking Oil on Biodiesel Production via Ester-transesterification in a Single Reactive Distillation. IOP Conf. Ser. Mater. Sci. Eng. **559**(1), 1 (2019). https://doi.org/10.1088/1757-899X/559/1/012014
26. Shah, K.A., Parikh, J.K., Maheria, K.C.: Optimization Studies and Chemical Kinetics of Silica Sulfuric Acid-Catalyzed Biodiesel Synthesis from Waste Cooking Oil. Bioenergy Res. **7**(1), 206–216 (2014). https://doi.org/10.1007/s12155-013-9363-y
27. dos Santos, R.C.M., et al.: Ethyl esters obtained from pequi and macaúba oils by transesterification with homogeneous acid catalysis. Fuel **259**(April), 2020 (2019). https://doi.org/10.1016/j.fuel.2019.116206